Diminished *Ret* expression compromises neuronal survival in the colon and causes intestinal aganglionosis in mice

Toshihiro Uesaka,[1] Mayumi Nagashimada,[1] Shigenobu Yonemura,[2] and Hideki Enomoto[1]

[1]Laboratory for Neuronal Differentiation and Regeneration and [2]Laboratory for Cellular Morphogenesis, RIKEN Center for Developmental Biology, Kobe, Japan.

Mutations in the *RET* gene are the primary cause of Hirschsprung disease (HSCR), or congenital intestinal aganglionosis. However, how *RET* malfunction leads to HSCR is not known. It has recently been shown that glial cell line–derived neurotrophic factor (GDNF) family receptor α1 (GFRα1), which binds to GDNF and activates RET, is essential for the survival of enteric neurons. In this study, we investigated *Ret* regulation of enteric neuron survival and its potential involvement in HSCR. Conditional ablation of *Ret* in postmigratory enteric neurons caused widespread neuronal death in the colon, which led to colonic aganglionosis. To further examine this finding, we generated a mouse model for HSCR by reducing *Ret* expression levels. These mice recapitulated the genetic and phenotypic features of HSCR and developed colonic aganglionosis due to impaired migration and successive death of enteric neural crest–derived cells. Death of enteric neurons was also induced in the colon, where reduction of *Ret* expression was induced after the period of enteric neural crest cell migration, indicating that diminished *Ret* expression directly affected the survival of colonic neurons. Thus, enteric neuron survival is sensitive to RET dosage, and cell death is potentially involved in the etiology of HSCR.

Introduction

Hirschsprung disease (HSCR), or intestinal aganglionosis, is one of the most common congenital disorders affecting the gastrointestinal tract and is characterized by the absence of enteric ganglia in the distal gut (1–5). Germline mutations in the *Ret* gene lead to the development of HSCR (6, 7). The *Ret* gene encodes the RET tyrosine kinase, which forms a receptor complex with GDNF family receptor α (GFRα) and mediates signaling of the glial cell line–derived neurotrophic factor (GDNF) family of ligands (GFLs) (8, 9). During enteric nervous system (ENS) development, RET and GFRα1 are expressed in ENS cells and their precursors, whereas GDNF is expressed in the gut mesenchyme (10). Consistent with this expression pattern and the close linkage between *Ret* mutations and HSCR, *Ret*-deficient mice fail to develop enteric ganglia (11). Because GDNF is chemoattractive for cells expressing *Ret* and *Gfra1* (12) and because *Ret*-deficient ENS precursors fail to migrate into the midgut, impaired migration of ENS precursors has been considered as a primary cause of HSCR. However, GDNF signaling also regulates the proliferation, differentiation, and survival of cells in the developing ENS (13–15), and it remains unclear whether impairment of any of these developmental processes by *Ret* mutations plays a crucial role in the etiology of HSCR.

Recent genetic studies have shown that GFRα1 plays an essential role in the survival of enteric neurons. Mice in which *Gfra1* gene function is conditionally disrupted during late gestation display widespread neuronal death specifically in the colon, leading to colon aganglionosis reminiscent of HSCR (16). In this study we have addressed whether *Ret* dysfunction induces enteric neuronal death and causes an HSCR phenotype by using 3 different in vivo strategies. First, by conditionally inactivating *Ret* gene function, we show that RET is essential for the survival of enteric neurons in the colon. Second, based on recent human genetic evidence suggesting the importance of RET dosage in the development of HSCR (17), we genetically engineered mice to express *Ret* at reduced levels. This resulted in generation of a mouse strain that exhibits crucial features of HSCR, including colon aganglionosis, incomplete penetrance with a sex bias, and the absence of kidney deficits. Using those mice as a HSCR model, we demonstrate that colon aganglionosis is established not only by impaired migration of ENS precursors but also by a failure of enteric neurons to survive in the colon. Third, by reducing the *Ret* expression levels in postmitotic enteric neurons, we provide evidence that reduction in *Ret* dosage directly affects the survival of colonic neurons in vivo. This study reveals that enteric neurons in the colon are intrinsically vulnerable to reduced RET dosage and implicates neuronal cell death in the etiology of HSCR.

Results

Physiological requirement of RET for the survival of enteric neurons in the colon. Enteric neurons in the colon fail to survive late gestation in the absence of GFRα1 (16). To examine whether RET is required for the survival of colonic neurons, we conditionally inactivated the function of the *Ret* gene. The *Ret* conditional allele was generated by inserting a gene cassette composed of floxed *Ret9* cDNA with intron polyA and followed by cyan fluorescent protein (CFP) cDNA (Figure 1A, referred to as floxed allele). The floxed allele was functional, as, unlike *Ret*-deficient mice, which die due to the absence of kidneys and enteric ganglia (11), $Ret^{fl/fl}$ mice were viable and grew to adulthood. On Cre treatment, the floxed allele was converted to a CFP-knockin allele that expressed CFP under the *Ret* promoter (Figure 1A). Crossing of $Ret^{fl/+}$ mice to β-actin Cre mice, in which Cre is deleted globally, resulted in the generation of $Ret^{CFP/+}$ mice, in which all *Ret*-expressing cells were labeled by

Nonstandard abbreviations used: CFP, cyan fluorescent protein; cKO, conditional KO; ENCDC, enteric neural crest–derived cell; ENS, enteric nervous system; GDNF, glial cell line–derived neurotrophic factor; GFRα1, GDNF family receptor α1; HSCR, Hirschsprung disease; 4-OHT, 4-hydroxytamoxifen.

Conflict of interest: The authors have declared that no conflict of interest exists.

Citation for this article: *J. Clin. Invest.* **118**:1890–1898 (2008). doi:10.1172/JCI34425.

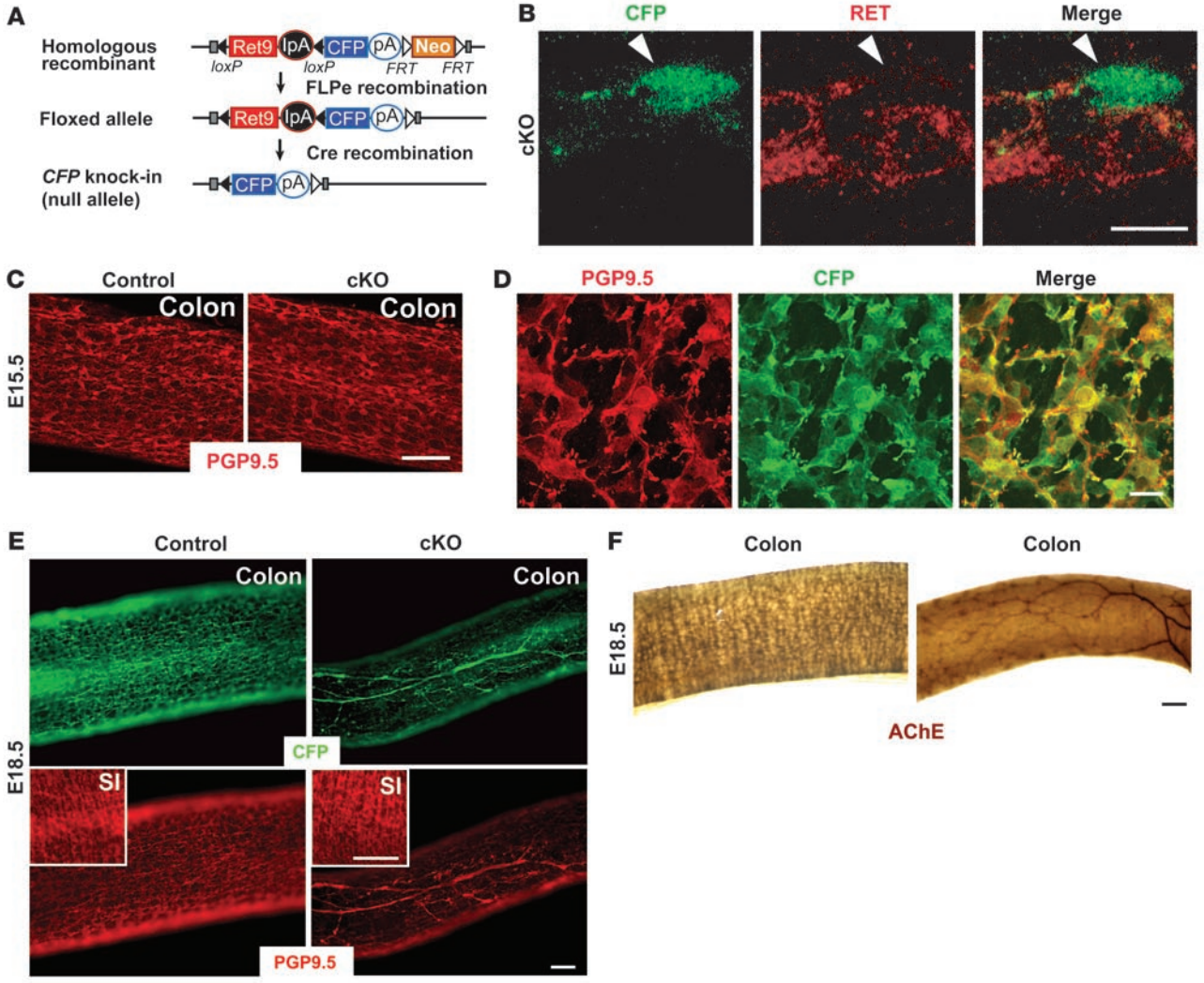

Figure 1

Inactivation of Ret depletes enteric neurons in the colon. (**A**) A gene cassette comprising floxed (black triangles, *loxP* sites) human *Ret9* cDNA (red box) with intron polyA (IpA, black ovals), CFP reporter (blue boxes), and neomycin resistance (Neo) expression cassette (orange box) flanked by FRT sites (open triangles) was introduced into exon 1 (gray boxes) of the mouse *Ret* locus (black lines) to generate a floxed *Ret* allele. Activation of Cre recombinase resulted in the removal of floxed *Ret9*, simultaneously generating CFP-knockin (*Ret*-null) allele. (**B**) RET antibody staining of cKO enteric plexus showing no RET immunoreactivity (red) in CFP$^+$ cells (green). Note the expression of RET (red) in neighboring unrecombined (CFP$^-$) cells. (**C**) PGP9.5 immunostaining of the distal colon in E15.5 control and cKO mouse fetuses before injection of 4-OHT. (**D**) 4-OHT–induced Cre recombination in enteric neurons. Administration of 4-OHT (0.5 mg per mouse) at E15.5 induced CFP expression in a large number of neurons in the colon. (**E**) Whole-mount CFP (upper panels) and PGP9.5 (lower panels) staining of the small intestine and colon from E18.5 control and cKO fetuses subjected to 4-OHT treatment at E15.5. Insets show ENS morphology in the small intestine (SI). (**F**) Whole-mount acetylcholinesterase (AChE) histochemical analysis of E18.5 colon 3 days after inactivation of *Ret*. Scale bars: 10 μm in **B**; 100 μm in **C**; 20 μm in **D**; 200 μm in **E** and **F**.

CFP (Supplemental Figure 1; supplemental material available online with this article; doi:10.1172/JCI34425DS1). The *Ret*-CFP knockin allele is null, as *Ret*$^{CFP/CFP}$ mice displayed a phenotype identical to that of *Ret*-deficient mice (Supplemental Figure 2) (11). To remove the floxed *Ret9* cassette at desired time points, we used mice ubiquitously expressing Cre-ER^{TM}, the activity of which can be induced by 4-hydroxytamoxifen (4-OHT). Induction of Cre activity by a low dose of 4-OHT treatment (0.2 mg per mouse) in conditional KO (cKO: *Ret*$^{fl/-}$*CAGGCre-ER*^{TM}) mice resulted in the emergence CFP$^+$ cells, all of which lacked RET immunoreactivity (Figure 1B; gut from an E15.5 fetus treated with 4-OHT at E13.5 shown as an example), validating the successful induction of *Ret*-deficient cells and their labeling by CFP in vivo. Development of the ENS proceeded normally in both cKO and control (*Ret*$^{fl/+}$ *CAGGCre-ER*^{TM}) fetuses (Figure 1C). We treated cKO and control fetuses with a higher dose of 4-OHT (0.5 mg per mouse) at E15.5, after the entire gut is furnished with nascent enteric ganglia, and the gut was examined at E18.5. In control colon, numerous CFP$^+$ ENS cells (Figure 1E, left) were found, and the recombination efficiency, which we estimated by dividing the number of CFP$^+$ cells by that of PGP9.5$^+$ cells, was more than 80% (Figure 1D). In cKO colon, very few enteric ganglion cells were detected by GFP

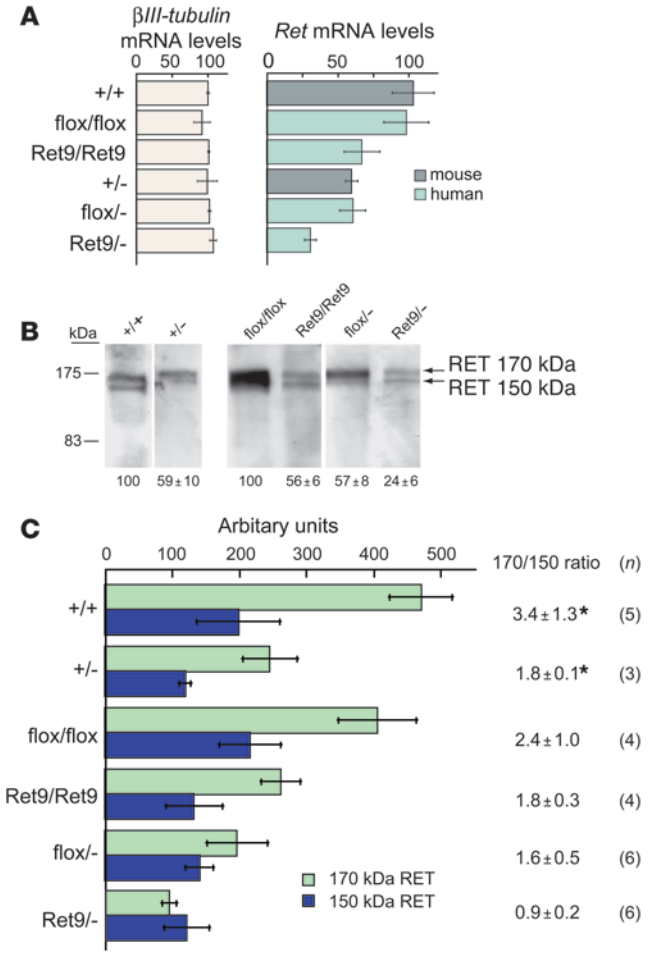

Figure 2
Quantitative analysis of *Ret* expression in enteric neurons. (**A**) Expression of *Ret* mRNA in the enteric plexus of small intestine at P0 was determined by real-time RT-PCR using human or mouse *Ret* primers. To estimate the total number of neurons in individual tissue samples, expression levels of βIII-tubulin mRNA were also determined. Results for each group was normalized to β-actin values. Error bars indicate SEM ($n = 3$). (**B**) Expression of RET protein in the enteric plexus of P0 $Ret^{+/+}$, $Ret^{fl/fl}$, $Ret^{9/9}$, $Ret^{+/-}$, $Ret^{fl/-}$, and $Ret^{9/-}$ mice. Protein extracts were immunoprecipitated with anti-RET antibody (C-19; Santa Cruz Biotechnology Inc.). Detection of mouse or human RET was done using antibody against the extracellular domain of RET (R&D Systems; or 12EXY, Santa Cruz Biotechnology Inc.). Results are shown separately for mouse RET (+/+ and +/–: left) and for human Ret9 (flox/flox, Ret9/Ret9, flox/–, and Ret9/–; right). Values for quantitated band intensities (sum of RET 170- and 150-kDA bands) are indicated below each lane (expression levels of RET in +/+ and flox/flox lanes were assigned as 100 for mouse and human RET, respectively). (**C**) The ratio of the glycosylated (170-kDA band) to the immature (150-kDa band) form is shown as mean ± SEM. *$P < 0.05$, statistically significant difference compared with $Ret^{9/-}$.

or PGP9.5 staining (Figure 1E, right). Acetylcholinesterase and PGP9.5 staining of the gut revealed nearly complete elimination of the enteric ganglia in the colon (Figure 1, E and F, right panels). No evident ENS cell loss was detected in the small intestine (Figure 1E, insets), revealing the specific dependence of colonic neurons on RET for their survival. This phenotype in cKO was almost identical to that observed in conditional GFRα1-knockout fetuses (16). These data indicate that RET is essential for the survival of colonic neurons specifically.

Generation of a mouse model of HSCR. Revealing that RET is physiologically required for the survival of colonic neurons, we set out to examine the potential involvement of *Ret*-dependent cell survival in ENS pathology, HSCR in particular. Although several *Ret* mutants have previously been reported to display aganglionosis (11, 18–23) and so resemble HSCR to some extent, several significant differences do exist in the phenotype of those animals and that of HSCR patients. For instance, in those *Ret* mutant mice, the aganglionic phenotype exhibits full penetrance and is associated with kidney deficits. In contrast, *Ret* mutation–associated HSCR is usually characterized by incomplete penetrance (1), and association of kidney malformation is extremely rare in HSCR (24). Understanding the physiology of RET in HSCR requires animal models that are more representative of genetic and clinical features of HSCR.

Recent genetic studies identified a common variant in a potential enhancer region of the *Ret* gene that is highly associated with HSCR (17). The enhancer activity is decreased by this variation in vitro. Based on the assumption that a reduction of *Ret* gene expression forms a critical basis for the development of HSCR, we generated a knockin allele that expresses *Ret9* cDNA under the *Ret* promoter (25). Because this knockin construct utilizes intron-less polyA, the levels of expression by *Ret9* allele ($Ret^{9/9}$) were reduced to approximately 60% of those of wild-type *Ret* or floxed *Ret9* ($Ret^{fl/fl}$) allele (Figure 2A). Wild-type, floxed *Ret*, *Ret9*, and the *Ret*-null allele were used to generate an allelic series of *Ret* mutant mice in which *Ret* expression levels were reduced to various extents (ranging from approximately one-third to normal levels in both mRNA and protein levels: Figure 2, A and B, respectively). Interestingly, the decrease in RET expression was accompanied by a dramatic reduction in the glycosylated mature form of RET (Figure 2C), suggesting that the activity of RET deteriorated to a greater extent than had been assumed from total RET expression levels. We found that the aganglionosis phenotype began to emerge when *Ret* expression was reduced to approximately one-third of its normal levels (Figure 3A; representative images taken from newborn mouse tissues, $Ret^{9/-}$ panels). Unlike *Ret*-deficient mice, which displayed nearly complete absence of the enteric ganglia throughout the entire gastrointestinal tract (Figure 3A, $Ret^{-/-}$), $Ret^{9/-}$ mice exhibited aganglionosis only in the colon, and the morphology of the enteric neuronal plexus in the small intestine of $Ret^{9/-}$ mice was indistinguishable from that of wild-type mice (Figure 3A, $Ret^{9/-}$ inset). Interestingly, other developmental processes that are critically dependent on *Ret* function (11, 26), including kidney formation (Supplemental Figure 2) and motor innervation to the latissimus dorsi muscle, remained intact in $Ret^{9/-}$ mice. Moreover, in $Ret^{9/-}$ mice, the aganglionosis phenotype occurred with incomplete penetrance (45.9%), and, in moderate cases where the length of the aganglionic segment did not exceed 3 mm, there was a tendency for males to be affected more frequently than females (58.6% versus 34.4%, respectively; $n = 61$) (Figure 3B and Table 1). Taken collectively, these data show that $Ret^{9/-}$ mice represent crucial features of HSCR and for that reason may serve as a valuable model system for understanding how the reduction of *Ret* expression causes aganglionosis in vivo.

Intestinal aganglionosis is established as the combinatorial result of deficits in cell migration and survival. To understand how ENS forma-

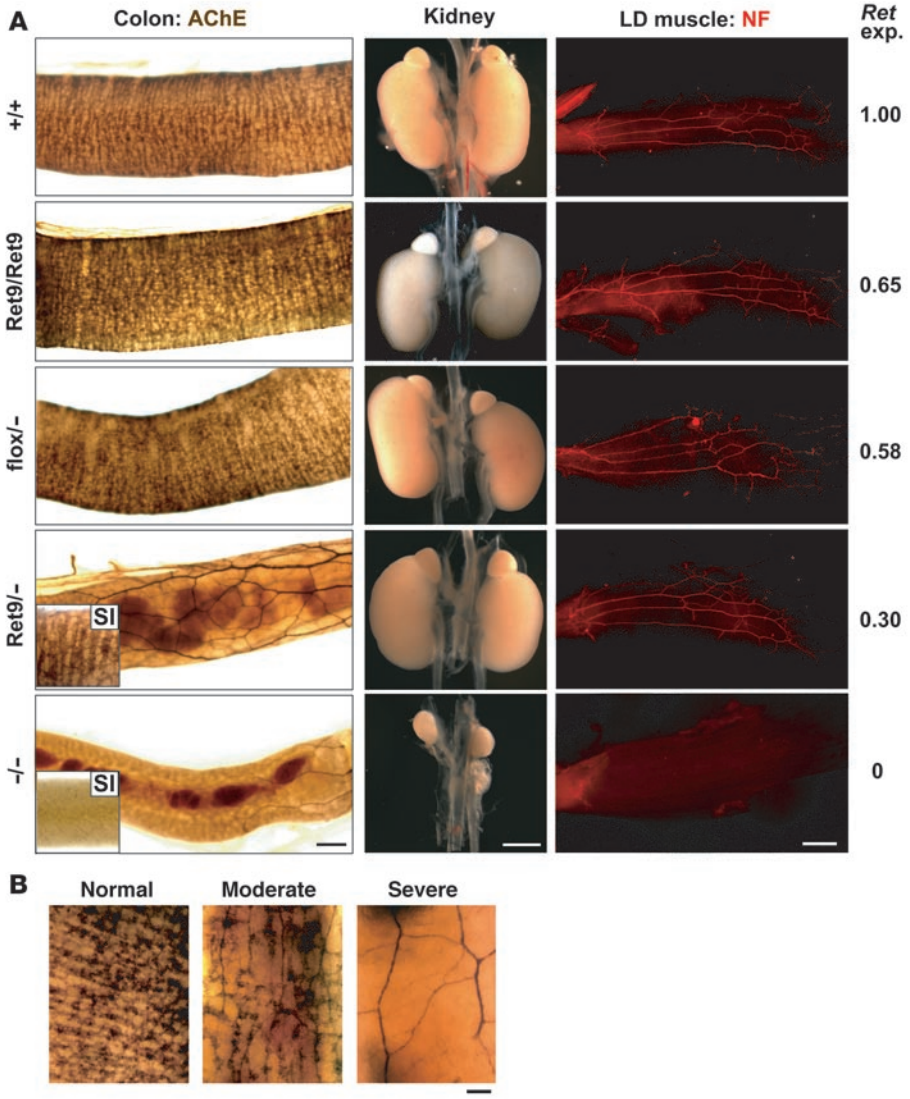

Figure 3
Reduced expression of *Ret* causes aganglionosis in the distal colon in vivo. (**A**) Dosage-dependent effects of *Ret* on the incidence and severity of aganglionosis in the gut. AChE staining of the colon (left panels), images of kidneys (middle panels), and neurofilament (NF) labeling of latissimus dorsi (LD) muscles (right panels) from $Ret^{+/+}$, $Ret^{9/9}$, $Ret^{fl/-}$, $Ret^{9/-}$, and $Ret^{-/-}$ newborn (P0) mice are shown. *Ret* expression levels (*Ret* exp.) were determined by real-time RT-PCR (see Figure 2). (**B**) Representative pictures of the gastrointestinal tracts of $Ret^{9/-}$ mice revealed by AChE histochemistry are shown. We refer to the reticulate pattern of enteric innervation with no aganglionic segment as normal. Cases were classified as severe when the length of the aganglionic segments in the entire colon exceeded 3 mm. Cases intermediate between normal and severe were classified as moderate. Scale bar: 200 μm in **A**; 100 μm in **B**.

tion is influenced by the reduction in RET dosage, we examined the developmental sequence of gut colonization by enteric neural crest–derived cells (ENCDCs) in $Ret^{9/CFP}$ and $Ret^{fl/CFP}$ fetuses, which expressed *Ret* at one-third and half of its normal levels, respectively (normalized values of *Ret* mRNA in $Ret^{9/CFP}$, $Ret^{fl/CFP}$, and wild-type were 0.009 [30.1%], 0.015 [51.7%], and 0.029 [100%]; percent values relative to wild-type expression levels shown in parentheses; $n = 3$; see Methods). During E9–E14, the vagal neural crest cells migrate down the gut mesenchyme in a craniocaudal direction. We first examined whether reduction of *Ret* expression influences the early phase of gut colonization by ENCDCs. In contrast to Ret-deficient mice, in which a delay in ENCDC migration is readily discernible at E9.5 (10), colonization of the gut by ENCDCs in $Ret^{9/CFP}$ or $Ret^{fl/CFP}$ fetuses was indistinguishable from that in wild-type fetuses until E10.5 (Supplemental Figure 4). We also examined whether *Ret* reduction affects the survival of ENCDCs (for analyzed region of embryo, see Figure 4A). As reported previously (15), many apoptotic figures were observed in the foregut of E10.5 $Ret^{CFP/CFP}$ fetuses (Figure 4D). However, no such abnormal death was detected in either $Ret^{9/CFP}$ or $Ret^{fl/CFP}$ fetuses (Figure 4, B and C). These data demonstrate that early ENS development is minimally affected even when *Ret* expression levels are reduced to one-third of its normal levels. The data also suggest that mechanisms underlying the development of intestinal aganglionosis are distinct between *Ret*-deficient and $Ret^{9/CFP}$ mice.

In $Ret^{fl/CFP}$ fetuses, the ENCDCs reached the cecum at E11.5, advanced into the middle portion of the hindgut at E12.5, and furnished the entire hindgut except the region close to the anal end at E13.5 (Figure 5, A–C). Migration of ENCDCs was completed by

Table 1
Incidence of aganglionosis in $Ret^{fl/-}$ and $Ret^{9/-}$ mice

Phenotype	$Ret^{fl/-}$	$Ret^{9/-}$	
		Males	Females
Normal (*n*)	19	12	21
Moderate (*n*)	0	11	3
Severe (*n*)	0	6	8
Incidence (%)	0	58.6	34.4

Total numbers of mice: $Ret^{fl/-}$, $n = 19$; $Ret^{9/-}$, $n = 61$ (male, 29; female, 32).

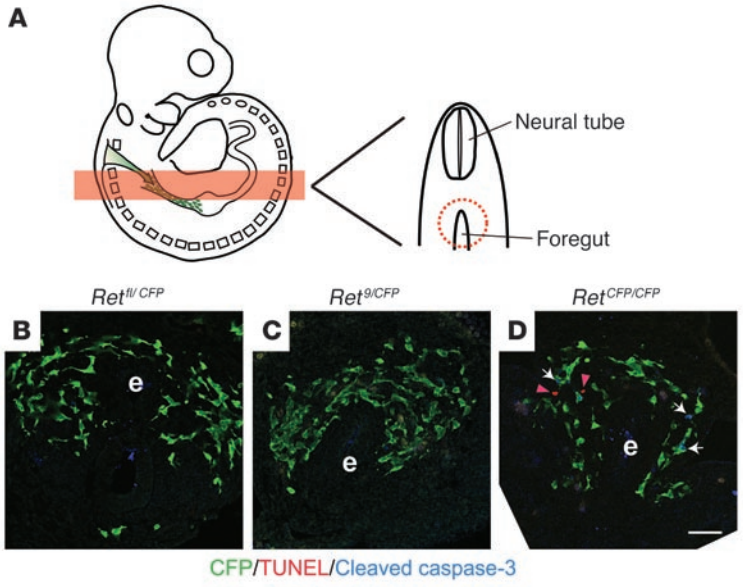

Figure 4
Apoptotic cell death of enteric neural crest in the foregut of fetuses in various *Ret* mutant fetuses. (**A**) A schematic depicting the position of the sectioning plane of E10.5 fetuses. (**B**–**D**) Detection of cell death by TUNEL combined with GFP and caspase-3 immunohistochemistry. Enteric neural crest cells were examined in transverse sections through the postotic region. TUNEL- (red, arrowheads) and cleaved caspase-3–positive cells (blue, arrows) were observed in $Ret^{CFP/CFP}$ fetuses (**D**, $n = 3$) but not in $Ret^{fl/CFP}$ (**B**, $n = 3$) or $Ret^{9/CFP}$ (**C**, $n = 6$) fetuses. e, endoderm of the foregut. Scale bars: 50 μm.

around E14 (27). Thus, the migratory behavior of ENCDCs in $Ret^{fl/CFP}$ fetuses was indistinguishable from that in wild-type fetuses, indicating that expression of *Ret9* at levels equivalent to 50% of those in wild-type RET is sufficient for normal ENCDC migration (Supplemental Figure 5). By contrast, $Ret^{9/CFP}$ ENCDCs displayed a slight delay at E11.5, especially at the levels where the migrating wave front advances into the hindgut (Figure 5A, arrowhead). During E12.5–E13.5, the delay in hindgut colonization by ENCDCs was greatly enhanced in all $Ret^{9/CFP}$ fetuses (Figure 5, B and C). Despite these changes, however, the ENCDCs colonized the entire small intestine, and the ENS of the midgut in those fetuses became indistinguishable from that in wild-type fetuses after E12.5.

In approximately half of $Ret^{9/CFP}$ fetuses, ENCDC colonization was not observed in the distal colon even at E15.5 (Supplemental Table 1), which stood in sharp contrast to the small intestine, where ENCDC colonization was always completed in all of those fetuses. Because RET-deficient enteric neurons in the colon fail to survive late gestation, we investigated whether abnormal neuronal cell death takes place in $Ret^{9/CFP}$ fetuses. We performed organ culture of the gut from E15.5 $Ret^{9/CFP}$ fetuses and examined CFP^+ ENCDCs by time-lapse fluorescence microscopy. In E15.5 $Ret^{9/CFP}$ fetal colon, which displayed a moderate delay in ENCDC colonization, many CFP^+ cells were readily identified, although the numbers of CFP^+ cells were noticeably fewer than those in control colon (Figure 6A, lower left). Surprisingly, during 6 hours of time-lapse observation, the majority of the CFP^+ cells in $Ret^{9/CFP}$ fetal colon disappeared in a progressive manner (Figure 6A, lower right, and Supplemental Movies 1 and 2). This disappearance of cells was detected in neither the small intestine of $Ret^{9/CFP}$ fetuses nor in the small or large intestine of control fetuses (Figure 6A, upper panels and data not shown). The gut regions displaying a progressive disappearance of CFP^+ cells were later examined by TuJ1 and Phox2b immunohistochemistry, which detects enteric neurons and their precursors, respectively. No cells were found remaining in those areas (Supplemental Figure 6), suggesting that the disappearance of CFP^+ cells reflects actual cell loss rather than loss of CFP expression. To further confirm this observation, we examined the morphology of ENCDCs by electron microscopy ($Ret^{fl/CFP}$, $n = 5$; $Ret^{9/CFP}$, $n = 10$). In $Ret^{fl/CFP}$ colon, most myenteric ganglion cells displayed round or ovoid nuclei with finely dispersed chromatin (Figure 6, B and C, left). ENCDCs in the colon of E15.5 $Ret^{9/CFP}$ fetuses were smaller and more sparsely distributed than those of control fetuses and displayed a number of degenerative changes (Figure 6B). Even in $Ret^{9/CFP}$ ganglia, whose structural integrity was relatively well preserved, a morphological alteration was already discernible in the nucleus: the nuclei were found to be abnormally indented, resulting in multilobular nuclei (Figure 6C, right). The results suggest that nuclear alterations occur initially. In $Ret^{9/CFP}$ enteric ganglia where cell loss or reduced ganglion size was recognized, cells were shrunken, while marginal heterochromatin became highly condensed at the periphery of the nuclear membrane (Figure 6D). Cells with heterophagosome-like vacuoles containing remnants of dead cells were often observed (Figure 6E). Despite these changes, the morphologies of mitochondria remained relatively intact in these cells, and no apoptotic figures were found (data not shown). Finally, the ultrastructure of ENCDCs appeared normal in the small intestine of $Ret^{9/CFP}$ fetuses (data not shown). The morphological attributes in the ENCDCs of $Ret^{9/CFP}$ fetuses were closely similar to those observed in degenerating ENCDCs of conditional mutants, in which the *Ret* or *Gfra1* gene function is disrupted during late gestation (16). These data demonstrate that significant numbers of ENCDCs undergo nonapoptotic cell death in $Ret^{9/CFP}$ colon.

Reduction in RET dosage directly affects enteric neuron survival in the colon. Because migration defects preceded enteric neuron death in $Ret^{9/CFP}$ fetuses, it was not clear whether enteric neuron death was caused directly by diminished *Ret* expression or indirectly as a secondary effect of delayed migration. To address this issue, we generated $Ret^{9/flox}$ mice carrying the *CAGGCre-ER*^{TM} transgene. In these animals, the *Ret* alleles ($Ret^{9/flox}$) allowed expression of *Ret* at approximately 80% of its normal levels (see Figure 2A). As expected, all of the $Ret^{9/flox}$ fetuses examined ($n = 8$) displayed normal ENS development; completion of enteric neural crest cell migration occurred at an expected developmental time period (E14.5; Figure 7A, middle), and successive formation of a dense reticular ENS network was observed throughout the entire gut (E15.5; Figure 7A, right). After the colonization of the entire gut by ENCDCs (E14.5

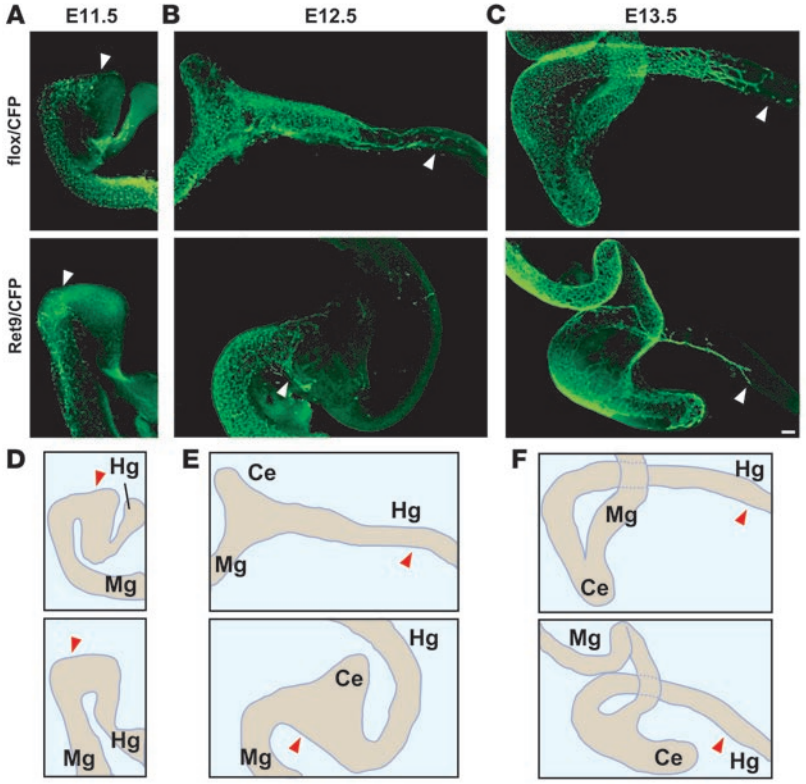

Figure 5
Delay in migration of enteric neural crest cells in $Ret^{9/CFP}$ mice. (**A**–**C**) CFP-positive neural crest cells (green) in the developing gut in $Ret^{fl/CFP}$ (top row) and $Ret^{9/CFP}$ mice (bottom row) at E11.5 (**A**), E12.5 (**B**), and E13.5 (**C**). At E12.5, the ENCDCs did not migrate beyond the cecum in any of the $Ret^{9/CFP}$ fetuses (n = 7). (**D**–**F**) Schematic drawing showing ENCDC migration (**A**–**C**). Arrowheads indicate the front of the migrating ENCDCs. Mg, midgut; Ce, cecum; Hg, hindgut. Scale bar: 100 μm.

or E15.5), $Ret^{9/flox}$ fetuses were administered 4-OHT in utero, which converted $Ret^{9/flox}$ to $Ret^{9/CFP}$ alleles, thereby reducing the *Ret* expression to one-third of wild-type levels in those fetuses. This conditional *Ret* reduction resulted in generation of fetuses with a severe depletion of ENCDCs (oligoganglionosis) at E18.5 (3 days after Cre activation) (Figure 7B). In the oligoganglionic gut, puncta of nerve fiber and cell body staining were frequently observed in the interganglionic spaces (Figure 7C, middle), suggesting an ongoing neurodegenerative process. As in $Ret^{9/CFP}$ fetuses, oligoganglionosis was only observed in the colon and exhibited incomplete penetrance with overall incidence of 17% (6 of 42) in 4-OHT–treated $Ret^{9/flox}$ fetuses (Figure 7D). The incidence of aganglionosis was lower in 4-OHT–treated $Ret^{9/flox}$ fetuses than in $Ret^{9/CFP}$ fetuses. Multiple factors could account for these differences, including Cre recombination efficiency and compensatory mechanisms to protect against cell death by neuronal differentiation (note that incidence of oligoganglionosis was slightly lower at E15.5 than at E14.5). Because of the relatively low incidence, we did not observe a statistically significant bias toward males, although there was such a tendency (male versus female incidence, 18.8% versus 6.7%, respectively). Nonetheless, this genetic manipulation provides compelling evidence that a reduction in RET dosage directly affects the survival of ENCDCs in the colon.

Discussion

Recent advances in mouse genetic engineering have allowed investigation of GDNF receptor function at specific developmental time periods (28–30), and we have recently shown that GFRα1, the high-affinity GDNF receptor, is crucial for enteric neuron survival during late gestation (16). This study provides, for the first time to our knowledge, genetic evidence that RET is essential for the survival of enteric neurons in the colon. Importantly, enteric neuron death is induced not only by loss of RET function but also by diminished RET expression. Since decreased RET expression is strongly implicated in HSCR, this study underscores the significance of cell death as one of developmental events linked to HSCR etiology.

In certain in vitro paradigms, RET has been known to function as a dependence receptor and induces apoptosis by activating caspases (31). In accordance with these findings, loss of *Ret* function results in somatotroph hyperplasia, which is interpreted to be caused by the absence of RET-derived pro-death signals (32). Since death of enteric neurons is induced by GFRα1 deficiency, it is important to assess whether enteric neuron death has any relevance to function of RET as a dependence receptor. In our observations, enteric neuron death was triggered in *Ret*-deficient enteric neurons nearly as efficiently as in GFRα1-deficient neurons that retain RET. This indicates that the pro-death action of RET suggested by the dependence receptor hypothesis is dispensable for triggering cell death in enteric neurons deprived of GDNF signaling. In addition, despite widespread death of enteric neurons induced by *Ret* or *Gfra1* inactivation, the death did not involve caspase activation and failed to display hallmarks of apoptosis morphologically. We therefore conclude that function of RET as a dependence receptor plays only a minor role, if any, in enteric neuron death.

In familial HSCR cases, the transmission of the disease shows a complex pattern of inheritance, and HSCR is thought to be multifactorial or oligogenic. Coding mutations in the *Ret* gene account for at least a fraction of patients (35% and 50% of sporadic and familial cases, respectively) (33). However, recent analysis of noncoding mutations in the *Ret* gene suggests that *Ret* mutations are in fact more frequent than has previously been thought and may even be considered necessary for all HSCR cases (17, 34). Of particular importance is the identification of such noncoding mutations in the enhancer region of the *Ret* gene, implying the significance of RET dosage in normal ENS development. Our study has shown for the first time to our knowledge that in mice, intestinal aganglionosis can develop simply by reduction of *Ret* gene expression to approximately one-third of its normal levels. Interestingly, these mice ($Ret^{9/-}$ mice) displayed incomplete penetrance of intestinal aganglionosis phenotype, with higher incidence in males than females. It should also be noted that this male preponderance was observed only in milder cases (shorter aganglionic segment). Moreover, kidney agenesis, which is consistently found in *Ret*-null mice but extremely rare in HSCR, was not observed in $Ret^{9/-}$ mice. Thus,

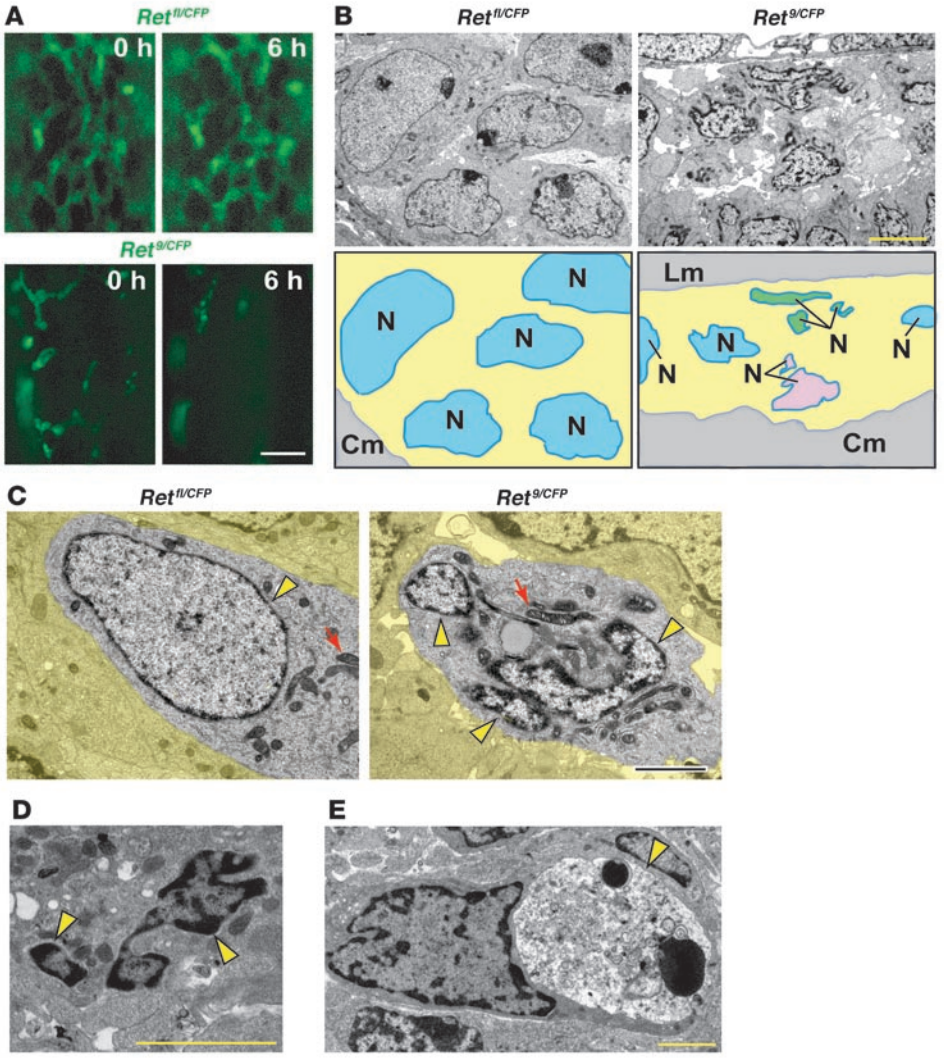

Figure 6
Progressive loss of enteric ganglion cells in *Ret*$^{9/CFP}$ fetal colon. (**A**) Loss of enteric ganglion cells in organ culture of E15.5 *Ret*$^{9/CFP}$ colon. (**B**) Electron microscopy of the myenteric ganglia in the colon from E15.5 *Ret*$^{fl/CFP}$ and *Ret*$^{9/CFP}$ fetuses. Many nuclei in *Ret*$^{9/CFP}$ fetal colon displayed abnormally constricted and irregularly shaped morphology (top right). Schematic drawings depict the location of the myenteric ganglia (yellow) and the positions of the nuclei in myenteric ganglion cells (indicated by N). Multiple nuclear profiles observed in a single cell plane are marked by pink and green. (**C**) Comparison of morphological characteristics of enteric ganglion cells between *Ret*$^{fl/CFP}$ and *Ret*$^{9/CFP}$ fetuses (E15.5). Cells with abnormally constricted nuclei were observed in *Ret*$^{9/CFP}$ fetuses (right). Arrows indicate mitochondria; arrowheads indicate nucleus. (**D**) A typical degenerating cell with enhanced heterochromatin condensation in *Ret*$^{9/CFP}$ distal colon. (**E**) Large vacuoles containing remnants of dying cells in *Ret*$^{9/CFP}$ distal colon (arrowheads). Lm, longitudinal muscle; Cm, circular muscle; N, nucleus. Scale bars: 20 μm in **A**; 5 μm in **B**; 2 μm in **C**–**E**.

phenotypic and genetic features of HSCR are more faithfully represented in *Ret*$^{9/-}$ mice than *Ret*-null mice. Our findings demonstrate that a failure in maintaining RET expression levels is central to the development of the disease and imply that, in multifactorial or oligogenic HSCR cases, mutations in genes other than *Ret* may converge to decrease *Ret* expression levels below the critical threshold.

In HSCR patients, coding mutations in the *Ret* gene are almost exclusively heterozygous, which led to the assumption that the reduction of *Ret* expression to 50% of its normal level is sufficient to cause HSCR in human. Because heterozygous *Ret*-deficient mice display normal ENS development, it has been speculated that the RET dosage required for normal ENS development is different in humans and mice. However, with recent evidence showing the presence of more than one mutation in the *Ret* gene in some HSCR patients (17), it seems reasonable to speculate that RET may be reduced to less than half of its normal level in at least a fraction of HSCR cases. Furthermore, not only the total RET expression but the levels of glycosylated RET (170-kDa RET: mature form) must also be taken into account, as we observed that decreased levels of total RET expression were associated with a dramatic reduction of 170-kDa RET expression (Figure 2C). It is therefore necessary to deduce whether the threshold levels of RET activity needed to maintain normal ENCDC migration and survival are conserved between mouse and human. Future quantitative analysis of RET in human subjects is required to address this issue. Mice with diminished *Ret* expression serve as a representative model for HSCR that occurs as an isolated trait, the most common form of HSCR.

Using *Ret*$^{9/-}$ mice as an HSCR model, we investigated how intestinal aganglionosis develops in these fetuses. In contrast to *Ret*-null fetuses in which enteric neuron precursors fail to colonize properly in the foregut and undergo apoptotic cell death at E9.5–E10.5 (15), ENS development proceeded normally in *Ret*$^{9/-}$ fetuses during the corresponding developmental time periods. This excluded the possibility that death of ENS precursors during early ENS development contributes to intestinal aganglionosis in *Ret*$^{9/-}$ fetuses. In later development, however, a delay in migration became discernible. Importantly, cell survival of ENCDCs was also impaired during late gestation (around E14.5), revealing a significant contribution of cell death to the development and progression of intestinal aganglionosis in *Ret*$^{9/-}$ fetuses. To examine whether enteric neuron death is a secondary effect of delayed migration, we reduced *Ret* expression after the completion of vagal neural crest migration. Widespread cell death could still be induced in this condition, indicating that diminished *Ret* expression directly affects the sur-

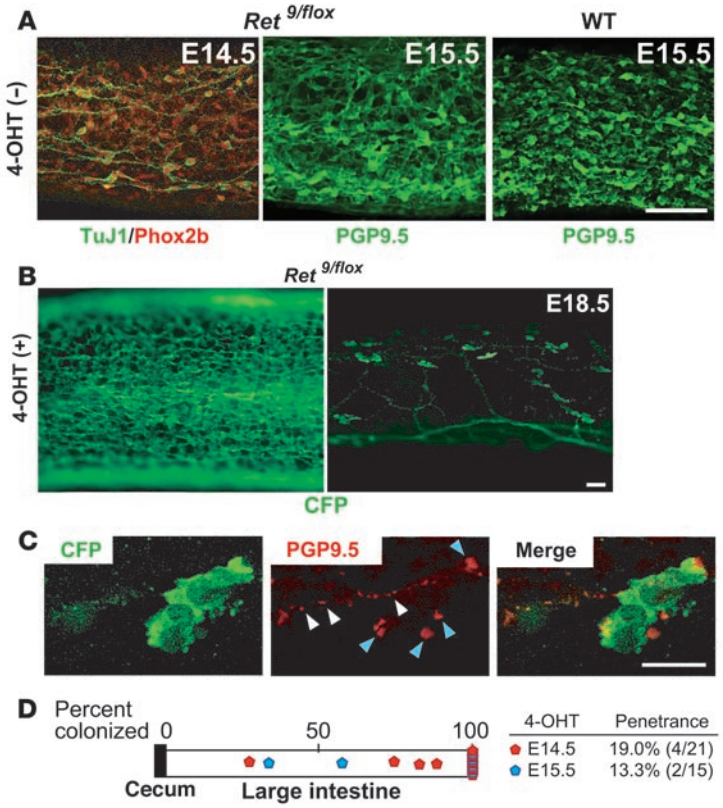

Figure 7
Conditional reduction of *Ret* depletes enteric neurons in the colon. (**A**) E14.5 and E15.5 *Ret*$^{9/flox}$*CAGGCre-ER*^{TM} distal colon before injection of 4-OHT. At E14.5, the entire colon was furnished with Phox2b^{+} cells (red), indicating that the entire gut is completely colonized by ENCDCs by this time period. The ENS formation in *Ret*$^{9/flox}$ was indistinguishable from that in wild-type. (**B**) Whole-mount preparation of the colon from E18.5 *Ret*$^{9/flox}$*CAGGCre-ER*^{TM} fetuses 3 days after administration of 4-OHT. Conditional reduction of Ret resulted in varying ENS phenotype ranging from apparently normal ENS formation (left) to colonic aganglionosis (right). (**C**) Neurons (blue arrowheads) and their neurites with signs of neurite degeneration (white arrowheads) in the aganglionic colon of *Ret*$^{9/flox}$ *CAGGCre-ER*^{TM} mice. (**D**) Schematic showing the extent of aganglionosis observed in E18.5 *Ret*$^{9/flox}$ fetuses. The beginning of the aganglionic segment (indicated by blue and red pentagons) was determined as the point where disruption of PGP9.5 staining was observed. Each blue and red pentagon represents 1 *Ret*$^{9/flox}$ mouse after injection of 4-OHT at E15.5 and E14.5, respectively. The numbers above the schematic indicate the percentage of gut colonization by neurons, where fully colonized hindgut was assigned as 100. Scale bar: 100 μm in **A** and **B**; 20 μm in **C**.

vival of enteric neurons. Based on these fi ndings, we propose that HSCR is caused not only by impaired migration of neural crest cells but by combined deficits in cell migration and survival. It will thus be important to assess the degree of contribution of cell death to the overall intestinal aganglionosis phenotype in both mice and humans in future studies in order to understand more fully the etiology of the disease and develop new therapeutic strategies.

Methods

Generation of conditional and Ret-knockin alleles. The conditional *Ret* allele (floxed *Ret9*) was generated by knocking a gene cassette composed of floxed human *Ret9* cDNA with SV40 intron polyA followed by a CFP reporter and a FRT-flanked neomycin resistance marker (Neo) into the first coding exon of the *Ret* gene. This strategy was identical to that described previously (25), except that instead of GFP, CFP was used as a reporter for the *Ret*-null allele conversion. *Ret9* allele was generated as described previously (35). For time-specific inactivation of *Ret*, floxed *Ret9* mice were crossed to mice ubiquitously expressing inducible Cre recombinase (*CAGGCre-ER*; The Jackson Laboratory) (36). Cre activity was induced by single intraperitoneal injection of 4-OHT (0.5 mg/100 μl; Sigma-Aldrich) into a pregnant mother carrying E14.5 or E15.5 fetuses. Mice used for this study were kept on a mixed 129/Sv × C57BL/6 background (>5 generations) and were cared for according to RIKEN Center for Developmental Biology institutional guidelines. All animal experiments were approved by the Animal Research Committee of the RIKEN Center for Developmental Biology and were carried out in accordance with RIKEN guidelines for animal and recombinant DNA experiments.

Genotyping. Primer sequences for genotyping of *Gfra1*$^{+/-}$, *Ret*^{flox}, *Ret*^{Ret9}, and *Ret*^{CFP} mice were: *Gfra1*$^{+/-}$, forward, 5′-CTTCCAGGTTGGGTCGGAACTGAACCC-3′; WT reverse, 5′-AGAGAGCTCAGCGTGCAGAGATC-3′; mutant reverse, 5′-CCAGGCAAAGCGCCATTCGCCATTCAGGCTGCG-3′; *Ret*^{flox}, forward, 5′-CGAGACCCGCCTGCTCCTCAACCGC-3′; reverse, 5′-CCTGCGGCGCCGGACGTCGCTTTCGCC-3′; *Ret*^{9}, forward, 5′-CGAGACCCGCCTGCTCCTCAACCGC-3′; WT reverse, 5′-AGCGCTAACTTCACCCCGGCCCCTACC-3′; mutant reverse, 5′-CAGCAGCAGCAGCAACAGCAGACGC-3′; *Ret*^{CFP}, forward, 5′-CGAGACCCGCCTGCTCCTCAACCGC-3′; WT reverse, 5′-CGAGACCCGCCTGCTCCTCAACCGC-3′; mutant reverse, 5′-TCGCCGGACACGCTGAACTTG-3′. The sex of the fetuses was determined by PCR (forward primer, 5′-CCTATTGCATGGACAGCAGCTTATG-3′; and reverse primer, 5′-GCATAGACATGTCTTAACATCTGTCC-3′), amplifying a 183-bp fragment of *Zfy1* located on the Y chromosome (37).

Real-time quantitative RT-PCR and Western blot analysis. Total RNA from myenteric plexus muscle layers of intestine was reverse-transcribed using Superscript II (Invitrogen), and *Ret* mRNA sequences were quantified by real-time PCR with 100 nM primers in Power SYBR Green PCR Master Mix (Applied Biosystems). Relative quantity values were calculated by the standard curve method. We used the quantity value of β-actin in each sample as a normalizing control. The primers used for *Ret* mRNA quantification were mouse *Ret*, forward: 5′-TTCCAGCATCAACTGCACTG-3′; reverse: 5′-GTCAGTGGCTACCACCGTGT-3′; human *RET*, forward: 5′-GTGTGAGTGGAGGCAAGGAG-3′; reverse: 5′-GTCCTGAGGGCAAATGTTGA-3′.

Melting curve analysis ensured exclusion of primer dimers from each analysis.

For Western blot analysis, protein extracts from the enteric plexus of small intestine were quantified by BCA assay (Pierce), and 150 μg of total proteins was subjected to immunoprecipitation with anti-RET antibody (C-19; Santa Cruz Biotechnology Inc.). Detection was done by antibody against the extracellular domain of RET (R&D Systems; or 12EXY, Santa Cruz Biotechnology Inc.). For quantification, Western blot films were scanned and subjected to densitometric analysis using ImageJ software (http://rsb.info.nih.gov/ij/).

Histological analysis and transmission electron microscopy. Immunohistochemistry, acetylcholinesterase histochemistry, and electron microscopy were performed as described previously (16, 38).

Time-lapse microscopy of gut organ culture. The gastrointestinal tract was dissected from each fetus and placed in tissue culture medium (DMEM containing 10% FBS, 2 mM glutamine and penicillin/streptomycin). The gut segments were placed across a V cut in a piece of Millipore filter paper (39). Time-lapse imaging was performed using an Olympus ZDC-IMAGE system.

Statistics. Statistical analysis was performed using the Mann-Whitney *U* test. Results are expressed as mean ± SEM.

Acknowledgments

We are indebted to Hitoshi Niwa for providing us with EB3 ES cells and Jean-François Brunet for anti-phox2b antibody. We also thank Yukinao Shibukawa, Kazuyo Misaki, members of the Enomoto laboratory and the Laboratory for Animal Resources and Genetic Engineering (LARGE) for their excellent technical assistance. This work was supported by RIKEN, MEXT "The Project for Realization of Regenerative Medicine" (H. Enomoto) and by a Grant-in-Aid for Young Scientists (B, 18790154) from the ministry of Education, Science, Sports, and Culture, Japan (T. Uesaka).

Received for publication November 5, 2007, and accepted in revised form March 5, 2008.

Address correspondence to: Hideki Enomoto, Laboratory for Neuronal Differentiation and Regeneration, RIKEN Center for Developmental Biology, 2-2-3 Minatojima-Minamimachi, Chuo-ku, Kobe, Hyogo 650-0047, Japan. Phone: 81-78-306-3099; Fax: 81-78-306-3089; E-mail: enomoto@cdb.riken.jp.

1. Badner, J.A., Sieber, W.K., Garver, K.L., and Chakravarti, A. 1990. A genetic study of Hirschsprung disease. *Am. J. Hum. Genet.* **46**:568–580.
2. Skinner, M.A. 1996. Hirschsprung's disease. *Curr. Probl. Surg.* **33**:389–460.
3. Parisi, M.A., and Kapur, R.P. 2000. Genetics of Hirschsprung disease. *Curr. Opin. Pediatr.* **12**:610–617.
4. Amiel, J., and Lyonnet, S. 2001. Hirschsprung disease, associated syndromes, and genetics: a review. *J. Med. Genet.* **38**:729–739.
5. Passarge, E. 2002. Dissecting Hirschsprung disease. *Nat. Genet.* **31**:11–12.
6. Edery, P., et al. 1994. Mutations of the RET proto-oncogene in Hirschsprung's disease. *Nature.* **367**:378–380.
7. Romeo, G., et al. 1994. Point mutations affecting the tyrosine kinase domain of the RET proto-oncogene in Hirschsprung's disease. *Nature.* **367**:377–378.
8. Airaksinen, M.S., and Saarma, M. 2002. The GDNF family: signalling, biological functions and therapeutic value. *Nat. Rev. Neurosci.* **3**:383–394.
9. Baloh, R.H., Enomoto, H., Johnson, E.M., Jr., and Milbrandt, J. 2000. The GDNF family ligands and receptors — implications for neural development. *Curr. Opin. Neurobiol.* **10**:103–110.
10. Natarajan, D., Marcos-Gutierrez, C., Pachnis, V., and de Graaff, E. 2002. Requirement of signalling by receptor tyrosine kinase RET for the directed migration of enteric nervous system progenitor cells during mammalian embryogenesis. *Development.* **129**:5151–5160.
11. Schuchardt, A., D'Agati, V., Larsson-Blomberg, L., Costantini, F., and Pachnis, V. 1994. Defects in the kidney and enteric nervous system of mice lacking the tyrosine kinase receptor Ret. *Nature.* **367**:380–383.
12. Young, H.M., et al. 2001. GDNF is a chemoattractant for enteric neural cells. *Dev. Biol.* **229**:503–516.
13. Chalazonitis, A., Rothman, T.P., Chen, J., and Gershon, M.D. 1998. Age-dependent differences in the effects of GDNF and NT-3 on the development of neurons and glia from neural crest-derived precursors immunoselected from the fetal rat gut: expression of GFRalpha-1 in vitro and in vivo. *Dev. Biol.* **204**:385–406.
14. Heuckeroth, R.O., Lampe, P.A., Johnson, E.M., and Milbrandt, J. 1998. Neurturin and GDNF promote proliferation and survival of enteric neuron and glial progenitors in vitro. *Dev. Biol.* **200**:116–129.
15. Taraviras, S., et al. 1999. Signalling by the RET receptor tyrosine kinase and its role in the development of the mammalian enteric nervous system. *Development.* **126**:2785–2797.
16. Uesaka, T., et al. 2007. Conditional ablation of GFRα1 in postmigratory enteric neurons triggers unconventional neuronal death in the colon and causes a Hirschsprung's disease phenotype. *Development.* **134**:2171–2181.
17. Emison, E.S., et al. 2005. A common sex-dependent mutation in a RET enhancer underlies Hirschsprung disease risk. *Nature.* **434**:857–863.
18. Asai, N., et al. 2006. Targeted mutation of serine 697 in the Ret tyrosine kinase causes migration defect of enteric neural crest cells. *Development* **133**:4507–4516.
19. Carniti, C., et al. 2006. The Ret(C620R) mutation affects renal and enteric development in a mouse model of Hirschsprung's disease. *Am. J. Pathol.* **168**:1262–1275.
20. de Graaff, E., et al. 2001. Differential activities of the RET tyrosine kinase receptor isoforms during mammalian embryogenesis. *Genes Dev.* **15**:2433–2444.
21. Jain, S., et al. 2004. Mice expressing a dominant-negative Ret mutation phenocopy human Hirschsprung disease and delineate a direct role of Ret in spermatogenesis. *Development.* **131**:5503–5513.
22. Jijiwa, M., et al. 2004. A targeting mutation of tyrosine 1062 in Ret causes a marked decrease of enteric neurons and renal hypoplasia. *Mol. Cell. Biol.* **24**:8026–8036.
23. Wong, A., et al. 2005. Phosphotyrosine 1062 is critical for the in vivo activity of the Ret9 receptor tyrosine kinase isoform. *Mol. Cell. Biol.* **25**:9661–9673.
24. Santos, H., Mateus, J., and Leal, M.J. 1988. Hirschsprung disease associated with polydactyly, unilateral renal agenesis, hypertelorism, and congenital deafness: a new autosomal recessive syndrome. *J. Med. Genet.* **25**:204–205.
25. Jain, S., Encinas, M., Johnson, E.M., Jr., and Milbrandt, J. 2006. Critical and distinct roles for key RET tyrosine docking sites in renal development. *Genes Dev.* **20**:321–333.
26. Haase, G., et al. 2002. GDNF acts through PEA3 to regulate cell body positioning and muscle innervation of specific motor neuron pools. *Neuron.* **35**:893–905.
27. Young, H.M., et al. 1998. A single rostrocaudal colonization of the rodent intestine by enteric neuron precursors is revealed by the expression of Phox2b, Ret, and p75 and by explants grown under the kidney capsule or in organ culture. *Dev. Biol.* **202**:67–84.
28. Jain, S., et al. 2006. RET is dispensable for maintenance of midbrain dopaminergic neurons in adult mice. *J. Neurosci.* **26**:11230–11238.
29. Kramer, E.R., et al. 2007. Absence of Ret signaling in mice causes progressive and late degeneration of the nigrostriatal system. *PLoS Biol.* **5**:e39.
30. Luo, W., et al. 2007. A hierarchical NGF signaling cascade controls Ret-dependent and Ret-independent events during development of nonpeptidergic DRG neurons. *Neuron.* **54**:739–754.
31. Bordeaux, M.C., et al. 2000. The RET proto-oncogene induces apoptosis: a novel mechanism for Hirschsprung disease. *EMBO J.* **19**:4056–4063.
32. Canibano, C., et al. 2007. The dependence receptor Ret induces apoptosis in somatotrophs through a Pit-1/p53 pathway, preventing tumor growth. *EMBO J.* **26**:2015–2028.
33. Hofstra, R.M., et al. 2000. RET and GDNF gene scanning in Hirschsprung patients using two dual denaturing gel systems. *Hum. Mutat.* **15**:418–429.
34. Griseri, P., et al. 2007. A common variant located in the 3′UTR of the RET gene is associated with protection from Hirschsprung disease. *Hum. Mutat.* **28**:168–176.
35. Enomoto, H., et al. 2001. RET signaling is essential for migration, axonal growth and axon guidance of developing sympathetic neurons. *Development.* **128**:3963–3974.
36. Hayashi, S., and McMahon, A.P. 2002. Efficient recombination in diverse tissues by a tamoxifen-inducible form of Cre: a tool for temporally regulated gene activation/inactivation in the mouse. *Dev. Biol.* **244**:305–318.
37. Kunath, T., et al. 2005. Imprinted X-inactivation in extra-embryonic endoderm cell lines from mouse blastocysts. *Development.* **132**:1649–1661.
38. Enomoto, H., et al. 1998. GFR α1-deficient mice have deficits in the enteric nervous system and kidneys. *Neuron.* **21**:317–324.
39. Young, H.M., et al. 2004. Dynamics of neural crest-derived cell migration in the embryonic mouse gut. *Dev. Biol.* **270**:455–473.